Available online at http://scik.org
Commun. Math. Biol. Neurosci. 2018, 2018:15
https://doi.org/10.28919/cmbn/3689
ISSN: 2052-2541

FINITE VOLUME SIMULATION OF TWO DIMENSIONAL CALCIUM DYNAMICS IN A HEPATOCYTE CELL INVOLVING BUFFERS AND FLUXES

YOGITA JAGTAP*, NEERU ADLAKHA

Applied Mathematics and Humanities Department,
Sardar Vallabhbhai National Institute of Technology, Surat 395007, India

Communicated by S. Shen

Abstract. The liver plays vital role in various activities like digestion, metabolism etc. in human body. The proper structure and functions of liver relies on its calcium homeostasis. The hepatocyte cell is a building block of liver. The calcium homeostasis in liver depends on intracellular calcium dynamics in a hepatocyte cell. The specific calcium levels are maintained for various activities in the hepatocyte cell. This calcium level depends on the processes of various influxes, effluxes and buffering mechanism. Any disturbances in these processes may lead to impaired function of the cell and cause disorder in function of liver. In this paper the mathematical model is proposed to study the effect of buffer and various fluxes like channel flux, leak and pump in a hepatocyte cell. The finite volume method for unsteady state case is implemented to obtain the solution of proposed problem in two dimensions. The effect of various physiological factors like concentration of exogenous and endogenous buffers, leak flux constant, channel conductance, pump rate, diffusion coefficient of medium on calcium concentration is demonstrated.

Keywords: calcium; buffer; fluxes; hepatocyte cell; finite volume method.

2010 AMS Subject Classification: 47H17, 47H05.

*Corresponding author

E-mail addresses: yogitajagtap7886@gmail.com

Received March 6, 2018

1. Introduction

Largest internal gland in human body is liver which is made up of parenchymal hepatocyte cells. Varieties of proteins necessary for initiation, sustentation and termination of basic cellular activities are secreted by hepatocyte cell. The functioning of liver is controlled by calcium signaling in hepatocyte cells. The concentration of free calcium ions plays crucial role in normal functioning of cell. Cell needs to keep calcium level inside the reference range from $0.1\mu M$ to $1\mu M$ to maintain normal calcium homeostasis [1]. The main source of calcium in hepatocyte cell is endoplasmic reticulum (ER). The calcium releases either from the gate of calcium channels embedded on ER membrane or small leakage through ER membrane. The calcium channels are abundant near apical surface of cell [2]. The released calcium from gate of calcium channel diffuses in cytosol of cell in presence of buffers to attain equilibrium calcium concentration towards basal surface of cell [3, 4]. The cyclic movement of calcium from ER to cytosol and viceversa is shown in Figure 1. The buffer binds with free calcium to minimize

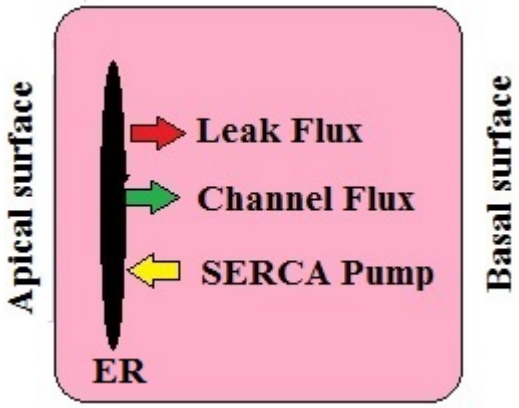

FIGURE 1. The calcium fluxes in a hepatocyte cell

the excess amount of free calcium. The SERCA pumps also flushes free calcium ions back into ER. Thus to maintain balanced level of calcium inside cell, there must be fine co-ordination in many physiological factors like quantity and type of buffers, channel fluxes, leakage, pumping rate, diffusion coefficient etc. [5].

In the past, many attempts has been made to study calcium signaling in cells like neuron [6, 7, 8, 9], fibroblast [10, 11], astrocyte [12, 13], acinar cell[14, 15, 16], oocyte [17, 18, 19],

myocyte [20, 21]. But very few attempts are made to study the calcium signaling in hepatocyte cell. In this paper an attempt has been made, to propose a mathematical model to study calcium dynamics in hepatocyte cell in presence of EGTA-Ethylene Glycol Tetra Acetic Acid and BAPTA-1,2-Bis(o-Amino Phenoxy) ethane- NNNN Tetra Acetic Acid, as exogeneous buffers and endogenous buffer.

2. Mathematical Model

The partial differential equation describing calcium dynamics in a hepatocyte cell in presence of excess buffer incorporating calcium fluxes is given by [22],

$$\frac{\partial C}{\partial t} = D_C\left(\frac{\partial^2 C}{\partial x^2}+\frac{\partial^2 C}{\partial y^2}\right)+(1+V)(V_{leak}+PV_{Chan})\left(\frac{C_T}{1+V}-C\right)$$

$$-P_R^{max}\frac{C^2}{C^2+K_{Pump}^2}-k_j^+[B_j]_\infty(C-C_\infty), \quad for \quad 0<x<20, \quad 0<y<20, \quad t>0 \tag{1}$$

The numerical values of biophysical constants are summarized in Table 1 [5, 22].

2.1. Initial condition

The background calcium concentration in hepatocyte cell before opening calcium channel gate is $0.1\mu M$ [1]. With this assumption initial condition can be framed as,

$$C_{t=0} = 0.1\mu M \tag{2}$$

2.2. Boundary condition

The calcium releasing channels are concentrated near apical surface of hepatocyte cell [2]. Therefore it is considered that calcium is released from a gate of calcium channel kept at node 3, situated near midway of apical surface at point (0, 10). Therefore the first boundary condition

TABLE 1. Numerical values of biophysical constants.

Symbol	Description	Numerical value
D_C	Diffusion coefficient	100-200 $\mu m^2/S$
V	Volume ratio of ER and cytosol	0.185
V_{leak}	Leak flux constant	$0.11S^{-1}$
P	Fraction of open channel	0-1
V_{Chan}	Channel conductance	$6S^{-1}$
P_R^{max}	Maximal pump rate	$0.9\mu M^{-1}S^{-1}$
K_{Pump}	Michaelis Menten Constant	$0.1\mu M$
C_∞	Equilibrium calcium concentration	$0.1\mu M$
k_1^+ for EGTA	Buffer association constant	$1.5\mu M^{-1}S^{-1}$
K_1 for EGTA	Dissociation constant	$0.2\mu M$
k_2^+ for Endogenous buffer	Buffer association constant	50 $\mu M^{-1}S^{-1}$
K_2 for Endogenous buffer	Dissociation constant	$10\mu M$
k_3^+ for BAPTA	Buffer association constant	600 $\mu M^{-1}S^{-1}$
K_3 for BAPTA	Dissociation constant	$0.17\mu M$
$[B]_T$	Total buffer concentration	50-150 μM

can be set by using Ficks law of diffusion as [5];

$$lim_{x\to 0,y\to 10} - D_C \frac{\partial C}{\partial x} = \sigma_C \tag{3}$$

Where, σ_C is influx of calcium from calcium channel.

The calcium concentration attains its equilibrium concentration $0.1\mu M$ far away from calcium channel i.e near basal surface of the hepatocyte cell. The hepatocyte cell is cubical in shape having length of approximately $20\mu m$ [1]. Therefore to set second boundary condition it is assumed that the distance required to attain equilibrium calcium concentration is length of hepatocyte cell.

$$lim_{x\to 20,y\to 20} C = C_\infty = 0.1\mu M \tag{4}$$

3. Solution by finite volume method

In the first step hepatocyte cell is discretized using uniform grid having 25 nodal points as shown in Figure 2.

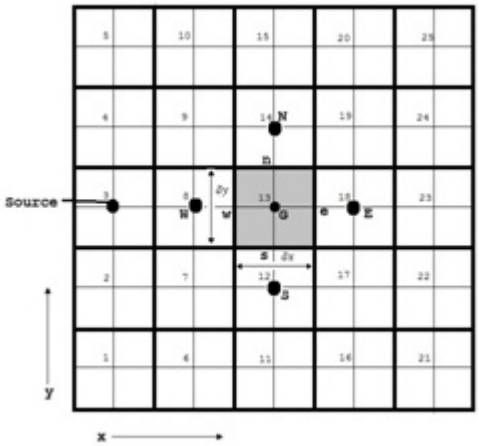

FIGURE 2. Two dimensional discretization of hepatocyte cell

For simplification we convert nonlinear partial differential Eq.(1) into linear form. For this we consider following two cases [20].

3.1. Case-I: $K_{Pump} >> C$

With this assumption we have,

$$\frac{C^2}{C^2+K_{Pump}^2} << \frac{C^2}{K_{Pump}^2} << \frac{C}{K_{Pump}} \tag{5}$$

Therefore Eq. (1) reduces to the form,

$$\frac{1}{D_C}\frac{\partial C}{\partial t} = \frac{\partial^2 C}{\partial x^2} + \frac{\partial^2 C}{\partial y^2} - a_1 C + b_1 \tag{6}$$

Where,

$$a_1 = \frac{(1+V)}{D_C}(V_{leak} + PV_{Chan}) + \frac{P_R^{max}}{D_C K_{Pump}} + \frac{k_j^+ [B_j]_\infty}{D_C}$$

$$b_1 = \frac{C_T}{D_C}(V_{leak} + PV_{Chan}) + \frac{k_j^+ [B_j]_\infty C_\infty}{D_C}$$

3.2. Case-II: $K_{Pump} << C$

Here we assume that, $K_{Pump} = \lambda C$ for $0 < \lambda < 1$ which gives,

$$\frac{C^2}{C^2 + K_{Pump}^2} = \frac{1}{1+\lambda^2} \tag{7}$$

With this approximation Eq. (1) reduces to the form,

$$\frac{1}{D_C}\frac{\partial C}{\partial t} = \frac{\partial^2 C}{\partial x^2} + \frac{\partial^2 C}{\partial y^2} - a_2 C + b_2 \tag{8}$$

Where,

$$a_2 = \frac{(1+V)}{D_C}(V_{leak} + PV_{Chan}) + \frac{k_j^+ [B_j]_\infty}{D_C}$$
$$b_2 = \frac{C_T}{D_C}(V_{leak} + PV_{Chan}) - \frac{P_R^{max}}{D_C}\frac{1}{1+\lambda^2} + \frac{k_j^+ [B_j]_\infty C_\infty}{D_C}$$

3.3. General equation for Case-I and Case-II

The Eq. (6) and Eq. (8) can be written in general form for case I and case II as,

$$\frac{1}{D_C}\frac{\partial C}{\partial t} = \frac{\partial^2 C}{\partial x^2} + \frac{\partial^2 C}{\partial y^2} - aC + b \tag{9}$$

Where, $a = a_1, b = b_1$ for case- I and $a = a_2, b = b_2$ for case- II.

Integrating Eq.(9) with respect to time and space over a control volume gives [23],

$$\int_t^{t+\Delta t}\int_{x_w}^{x_e}\int_{y_s}^{y_n}\frac{1}{D_C}\frac{\partial C}{\partial t}dydxdt = \int_t^{t+\Delta t}\int_{x_w}^{x_e}\int_{y_s}^{y_n}\left(\frac{\partial^2 C}{\partial x^2} + \frac{\partial^2 C}{\partial y^2} - aC + b\right)dydxdt \tag{10}$$

Solving space integration we get,

$$\frac{\delta x \delta y}{D_C}\int_t^{t+\Delta t}\frac{\partial C_G}{\partial t}dt = \int_t^{t+\Delta t}\left[\left(\frac{\partial C}{\partial x}\right)_e - \left(\frac{\partial C}{\partial x}\right)_w + \left(\frac{\partial C}{\partial y}\right)_n - \left(\frac{\partial C}{\partial y}\right)_s\right]dt$$
$$-a\delta x\delta y\int_t^{t+\Delta t} C_G dt + b\delta x\delta y\int_t^{t+\Delta t} dt \tag{11}$$

Now for solving time integral we use weighted parameter θ which lies between 0 to 1.

$$\frac{\delta x\delta y}{D_C}[C_G - C_G^0] = \theta\left[\frac{C_E - C_G}{\delta x} - \frac{C_G - C_W}{\delta x} + \frac{C_N - C_G}{\delta y} - \frac{C_G - C_S}{\delta y}\right]\Delta t$$
$$+(1-\theta)\left[\frac{C_E^0 - C_G^0}{\delta x} - \frac{C_G^0 - C_W^0}{\delta x} + \frac{C_{N^0} - C_G^0}{\delta y} - \frac{C_G^0 - C_S^0}{\delta y}\right]\Delta t$$
$$-a\delta x\delta y[\theta C_G - (1-\theta)C_G^0]\Delta t + b\delta x\delta y\Delta t \tag{12}$$

Where the values of C at time t are super scripted with 0. Rearranging Eq.(12) gives,

$$\left[\frac{\delta x\delta y}{D_C\Delta t}+\frac{\theta}{\delta x}+\frac{\theta}{\delta x}+\frac{\theta}{\delta y}+\frac{\theta}{\delta y}+a\theta\delta x\delta y\right]C_G$$
$$=\left[\frac{\delta x\delta y}{D_C\Delta t}-\frac{(1-\theta)}{\delta x}-\frac{(1-\theta)}{\delta x}-\frac{(1-\theta)}{\delta y}+\frac{(1-\theta)}{\delta y}-a(1-\theta)\delta x\delta y\right]C_G^0$$

(13)
$$+\frac{\theta C_E+(1-\theta)C_E^0}{\delta x}+\frac{\theta C_W+(1-\theta)C_W^0}{\delta x}+\frac{\theta C_N+(1-\theta)C_N^0}{\delta y}+\frac{\theta C_S+(1-\theta)C_S^0}{\delta y}+b\delta x\delta y$$

To apply Crank Nicolson method we put $\theta=1/2$ in Eq.(13),

$$\left[\frac{\delta x\delta y}{D_C\Delta t}+\frac{1}{2}\left(\frac{1}{\delta x}+\frac{1}{\delta x}+\frac{1}{\delta y}+\frac{1}{\delta y}\right)+\frac{1}{2}a\delta x\delta y\right]C_G$$
$$=\left[\frac{\delta x\delta y}{D_C\Delta t}-\frac{1}{2}\left(\frac{1}{\delta x}+\frac{1}{\delta x}+\frac{1}{\delta y}+\frac{1}{\delta y}\right)-\frac{1}{2}a\delta x\delta y\right]C_G^0$$

(14)
$$+\frac{1}{2}\frac{C_E+C_E^0}{\delta x}+\frac{1}{2}\frac{C_W+C_W^0}{\delta x}+\frac{1}{2}\frac{C_N+C_N^0}{\delta y}+\frac{1}{2}\frac{C_S+C_S^0}{\delta y}+b\delta x\delta y$$

For all internal nodes, Eq.(14) can be put in the form,

(15) $$a_GC_G=a_G^0C_G^0+\frac{a_E}{2}[C_E+C_E^0]+\frac{a_W}{2}[C_W+C_W^0]+\frac{a_N}{2}[C_N+C_N^0]+\frac{a_S}{2}[C_S+C_S^0]+S_u$$

Where,

$$a_G=\left[\frac{\delta x\delta y}{D_C\Delta t}+\frac{1}{2}(a_E+a_W+a_N+a_s)+\frac{1}{2}a\delta x\delta y\right]$$
$$a_G^0=\left[\frac{\delta x\delta y}{D_C\Delta t}-\frac{1}{2}(a_E+a_W+a_N+a_s)-\frac{1}{2}a\delta x\delta y\right]$$
$$a_E=a_W=\frac{1}{\delta x}$$
$$a_N=a_S=\frac{1}{\delta y}$$
$$S_u=b\delta x\delta y$$

Incorporating first boundary condition at node 3 by setting, $C_W=\sigma_C$ we get,

(16) $$a_GC_G=a_G^0C_G^0+\frac{a_E}{2}[C_E+C_E^0]+\frac{a_N}{2}[C_N+C_N^0]+\frac{a_S}{2}[C_S+C_S^0]+S_u$$

Where,

$$a_G=\left[\frac{\delta x\delta y}{D_C\Delta t}+\frac{1}{2}(a_E+a_N+a_s)+(\frac{1}{\delta x}+\frac{1}{2}a\delta x\delta y)\right]$$
$$a_G^0=\left[\frac{\delta x\delta y}{D_C\Delta t}-\frac{1}{2}(a_E+a_N+a_s)-(\frac{1}{\delta x}+\frac{1}{2}a\delta x\delta y)\right]$$
$$a_E=\frac{1}{\delta x}$$
$$a_N=a_S=\frac{1}{\delta y}$$

$$S_u = (\frac{2\sigma_C}{\delta x} + b\delta x\delta y)$$

Incorporating second boundary condition at node 1 by setting $C_\infty = 0.1$ and $a_W = a_S = 0$ for cutting link with boundary we get,

$$a_G C_G = a_G^0 C_G^0 + \frac{a_E}{2}[C_E + C_E^0] + \frac{a_N}{2}[C_N + C_N^0] + S_u \tag{17}$$

Where,

$$a_G = \left[\frac{\delta x\delta y}{D_C\Delta t} + \frac{1}{2}(a_E + a_N) + (\frac{1}{\delta x} + \frac{1}{\delta y} + \frac{1}{2}a\delta x\delta y)\right]$$
$$a_G^0 = \left[\frac{\delta x\delta y}{D_C\Delta t} - \frac{1}{2}(a_E + a_N) - (\frac{1}{\delta x} + \frac{1}{\delta y} + \frac{1}{2}a\delta x\delta y)\right]$$
$$a_E = \frac{1}{\delta x}$$
$$a_N = \frac{1}{\delta y}$$
$$S_u = (\frac{2C_B}{\delta x} + \frac{2C_B}{\delta y} + b\delta x\delta y)$$

Similarly boundary condition can be incorporated at nodes 5, 21 and 25. The system of linear algebraic equations obtained in Eq.(15) to Eq. (17) at each time step can be put in matrix form as follows;

$$[A]_{25\times 25} * [C]_{25\times 1} = [B]_{25\times 1} \tag{18}$$

Where, [A] is system matrix, [C] is concentration vector and [B] is constant vector. The Eq.(18) is solved at each iteration to obtain solution vector $[C]_{25\times 1}$. The numerical simulations has been done in MATLAB 2014a, to obtain the solution.

4. Results and Discussion

The effect of change in EGTA buffer concentration i.e. [EGTA] on calcium concentration is shown in Figure 3 for case-I and Figure 4 for case-II. In both cases it is observed that with increase in value [EGTA] from $50\mu M$ to $150\mu M$ the concentration of free calcium decreases simultaneously. In case-I where $K_{Pump} >> C$ concentration of free calcium is less in comparison with that for case-II where $K_{Pump} << C$. This is because of larger value of K_{Pump} sequesters maximum amount of calcium back into ER. The equilibrium calcium concentration is slightly higher in case-II.

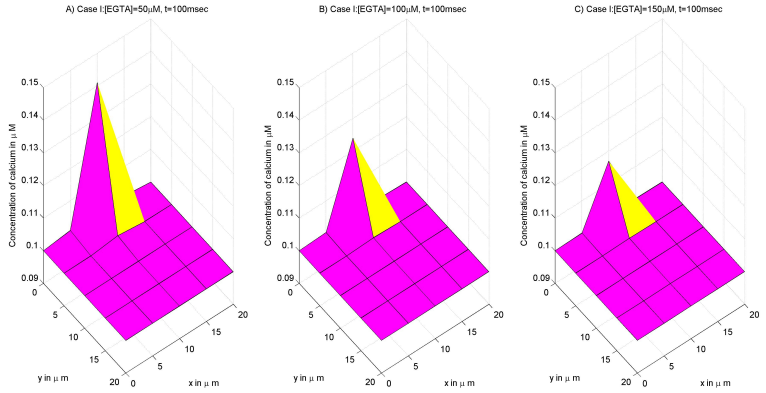

FIGURE 3. Case-I. Variation of calcium in space in presence of EGTA buffer at time t=100 ms

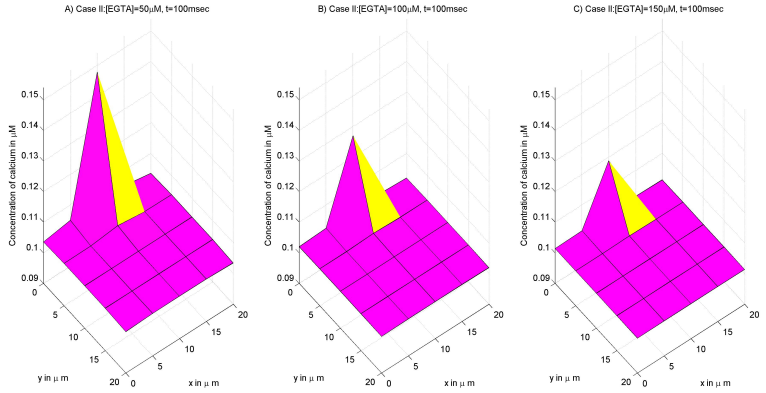

FIGURE 4. Case-II. Variation of calcium in space in presence of EGTA buffer at time t=100 ms

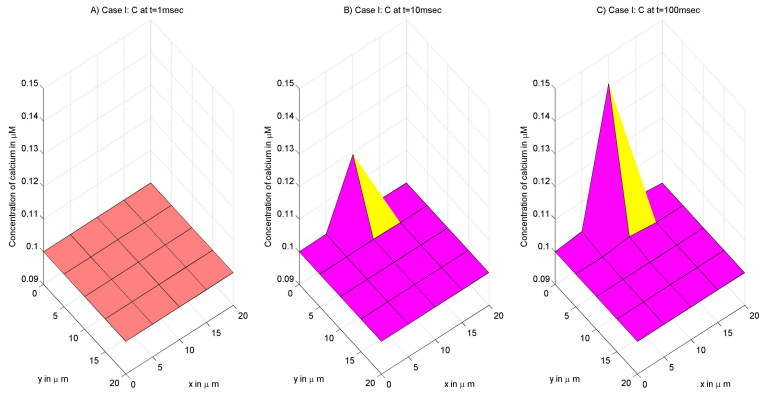

FIGURE 5. Case-I. Variation of calcium in space at different time step in presence of [EGTA]= 50 μM

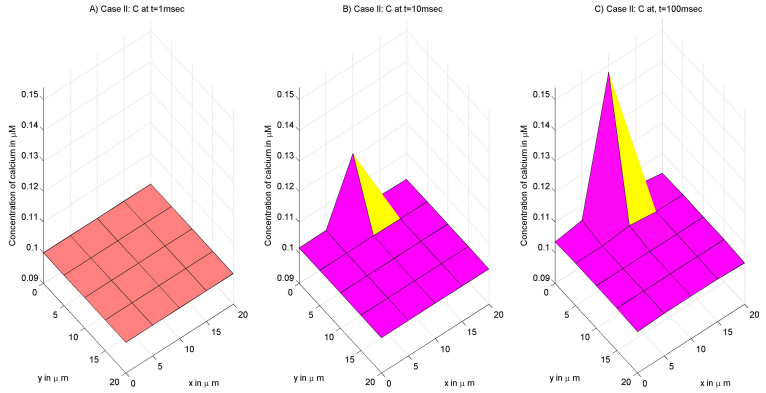

FIGURE 6. Case-II. Variation of calcium in space at different time step in presence of [EGTA]= 50 μM

The calcium concentration in hepatocyte cell in presence of 50 μM EGTA concentration at different time level in both cases is shown in Figure 5 and Figure 6. The concentration of calcium increases gradually from 0.1 μM and attains steady state concentration in 100 *msec*. It can be seen that near gate of calcium channel the calcium concentration is having peak value. It decreases with distances away from source.

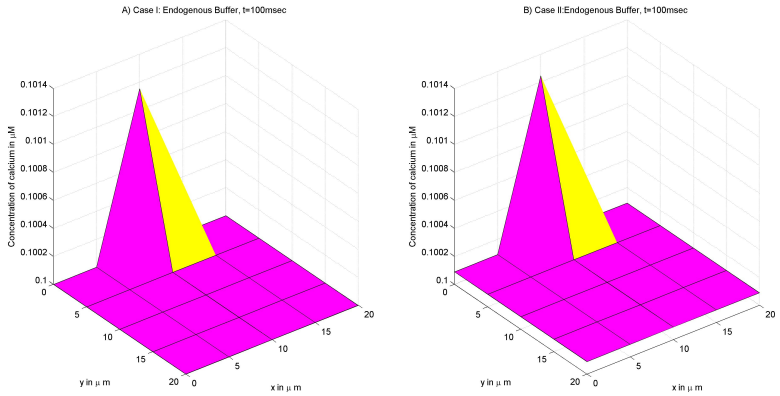

FIGURE 7. Case-I and II. Variation of calcium in space at time = 100 msec in presence of [Endogenous buffer]= 50 μM

The profile of calcium concentration in presence of endogenous buffer is as shown in Figure 7 for case-I and case-II respectively for steady state. The calcium concentration in presence of endogenous buffer is much less than that in case of EGTA buffer. This is because of high

binding capacity of endogenous buffer. It captures free calcium ions instantly as compared to EGTA.

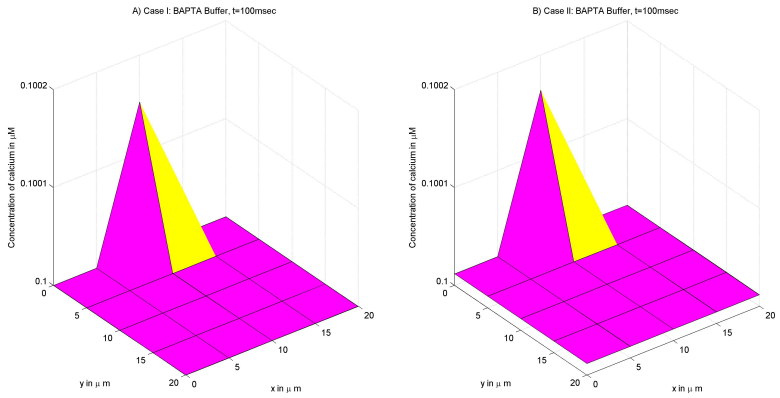

FIGURE 8. Case-I and II. Variation of calcium in space at time = 100 msec in presence of [BAPTA]= 50 μM

In Figure 8 the profile of calcium concentration is shown in presence of BAPTA buffer at steady state. The nodal calcium concentration is less as compared to the cases of other buffers. BAPTA buffer has highest association rate constant than that of other considered buffers. Therefore it binds with calcium ions as soon as they released from channel gate. This leads to decrease in value of nodal calcium concentration.

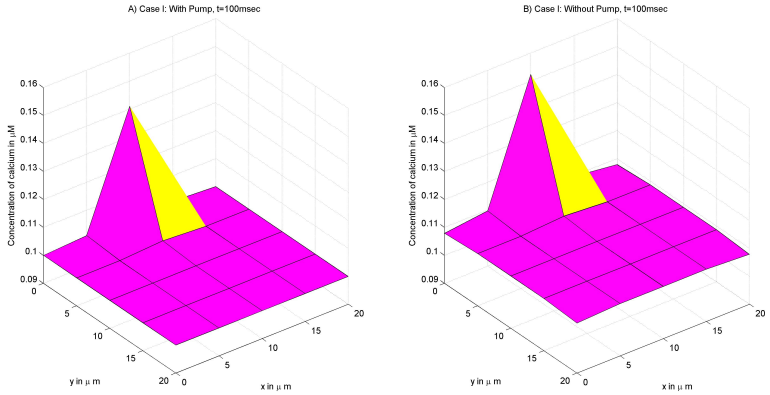

FIGURE 9. Case-I. Variation of calcium in space at time = 100 msec with pump and without pump

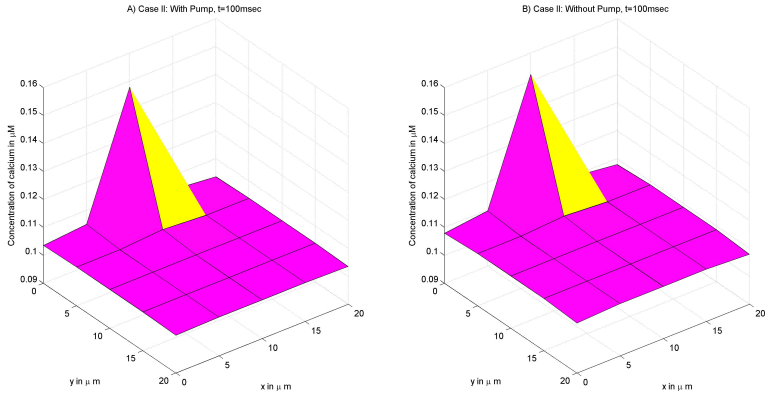

FIGURE 10. Case II. Variation of calcium in space at time = 100 msec with pump and without pump

Figure 9 and Figure 10 are plotted to study effect of SERCA pump on cytosolic calcium concentration in case- I and case-II respectively in presence of EGTA buffer. It is observed that in absence of pump the calcium concentration is higher at each node. In this condition only present buffers bind with free calcium ion to minimize unnecessary increase of calcium concentration.

Figure 11 shows the difference in values of calcium concentration with pump and without

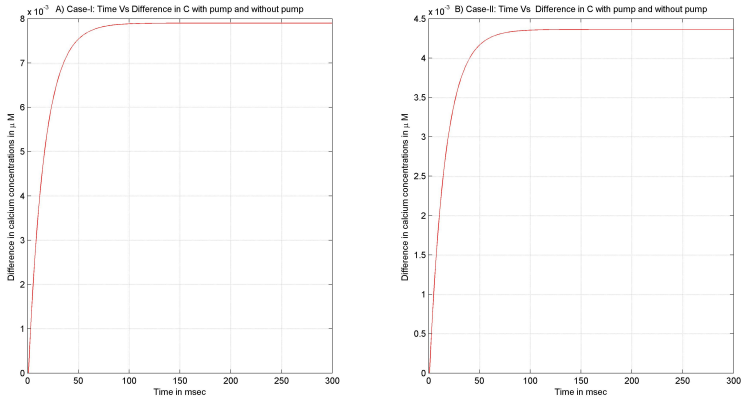

FIGURE 11. The difference in calcium concentration with pump and without pump with respect to time

pump. It is observed that this difference increases sharply with time upto 100msec and after that it increases gradually and becomes almost constant. This is due to the equilibrium among the processes which have been achieved by the cell after 100msec. It is also observed that the

difference is maximum in case- I than in case-II. This is because in case-I K_{pump} is much higher than that in case II.

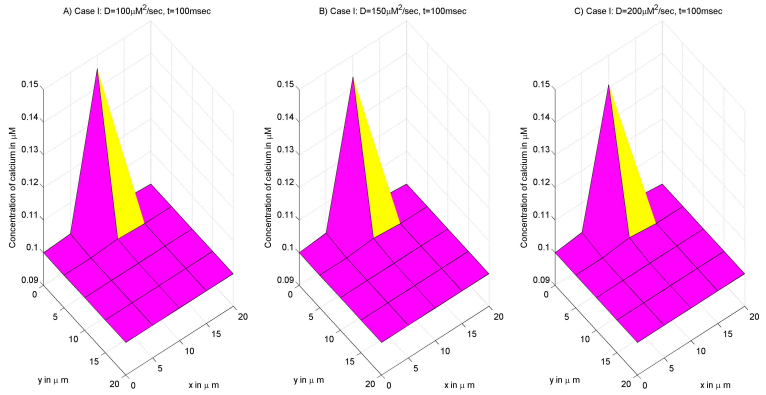

FIGURE 12. Case-I. Variation of calcium in space at time = 100 msec with increase in value of diffusion coefficient

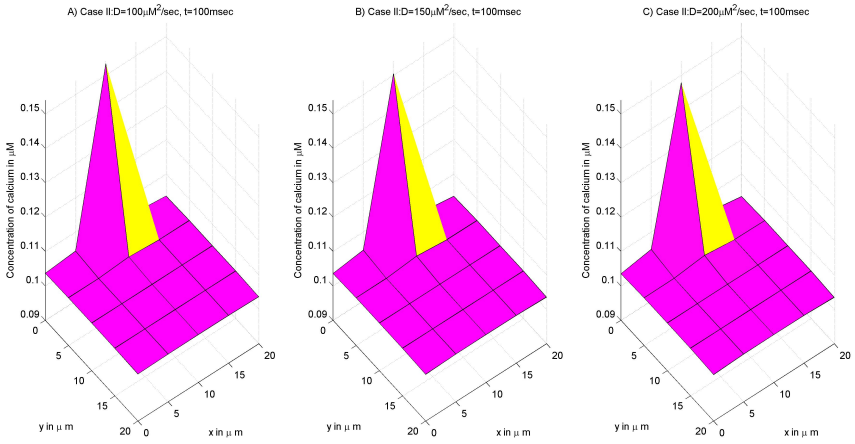

FIGURE 13. Case II. Variation of calcium in space at time = 100 msec with increase in value of diffusion coefficient

To study effect of diffusion coefficient on calcium profile the numerical simulations are done by assuming different values of diffusion coefficient as shown in Figure 12 and Figure 13 respectively for case-I and case- II. It can be seen that the increase in value of diffusion coefficient spontaneously decreases value of calcium concentration. This is because the increased value of

diffusion coefficient transports more calcium ions from one part of cell to other part. Which results in decrease in accumulated nodal calcium concentration.

5. Conclusion

A finite volume model is proposed and successfully employed to study effect of excess buffers like EGTA buffer, endogenous buffer, BAPTA buffer, channel flux, leak and pump on variation of calcium concentration in a hepatocyte cell for two dimensional case. On the basis of results obtained, it is concluded that, the BAPTA buffer has more significant effect than EGTA and endogenous buffer in reducing the calcium concentration in a hepatocyte cell. Thus quantity and type of buffers play an vital role in reducing calcium concentration under various condition in which the calcium concentration becomes high in the cell during particular activity. Also the SERCA pump helps to collect calcium ions back into ER to maintain balanced range of calcium. The high levels of calcium concentration in the cell for longer periods can cause cell death. Thus these buffers and SERCA pumps protect the cell in such conditions by reducing the calcium concentration. The results obtained here are in agreement with biophysical facts, however no such experimental results are available for comparison. The finite volume method has proved to be quite versatile in incorporating the parameters and obtaining interesting results. The information of spatiotemporal calcium profiles under various conditions can be generated from such models and can be useful to clinical applications in detection and treatment of diseases related to liver.

Conflict of Interests

The authors declare that there is no conflict of interests.

Acknowledgements

Authors are thankful to department of biotechnology, Delhi for providing infrastructure facility to carry out this work.

REFERENCES

[1] Dupont G, Swillens S, Clair C, Tordjmann T, Hierarchical organization of calcium signals in hepatocytes: from experiments to models, Biochimica et Biophysica Acta (BBA)-Molecular Cell Research, 1498(2000), 104-114.

[2] Amaya MJ, Nathanson MH, Calcium signaling in the liver, Comprehensive Physiology 3(2013), 515-539.

[3] Thomas AP, Bird GSTJ, Hajnoczky G, Gaspers R, Spatial and temporal aspects of cellular calcium signaling, FASEB J. 10(1996), 1505-1517.

[4] Pochet R, Donato R et.al, Calcium: The molecular basis of calcium action in biology and medicine, Springer Science & Business Media, 3(2011) 73-94.

[5] Keener JP, Sneyd J, Mathematical physiology, Springer (1998), 309-313.

[6] Tewari S, Pardasani KR, Finite element model to study two dimensional unsteady state cytosolic calcium diffusion in presence of excess buffers, IAENG Int. J. Appl. Math. 40(2010), 108-112.

[7] Tewari S, Pardasani KR, Finite difference model to study the effects of Na+ influx on cytosolic Ca 2+ diffusion, Int. J. Biol. Med. Sci. 1(2009), 205-210.

[8] Jha A, Adlakha N, Two-dimensional finite element model to study unsteady state Ca 2+ diffusion in neuron involving ER LEAK and SERCA, Int. J. Biomath. 89(2015), 1550002.

[9] Jha A, Adlakha N, Finite element model to study the effect of exogenous buffer on calcium dynamics in dendritic spines, Int. J. Model. Simul. Sci. Comput. 5(2014), 1350027.

[10] Kotwani M, Adlakha N, Modeling of endoplasmic reticulum and plasma membrane Ca 2+ uptake and release fluxes with excess buffer approximation (EBA) in fibroblast cell, Int. J. Comput. Materials Sci. Eng. 6(2017), 1750004.

[11] Kotwani M, Adlakha N, Finite element model to study the effect of buffers, source amplitude and source geometry on spatio-temporal calcium distribution in fibroblast cell, J. Med. Imaging Health Inf. 4(2014), 840-847.

[12] Jha BK, Adlakha N, Mehta MN, Two-dimensional finite element model to study calcium distribution in astrocytes in presence of vgcc and excess buffer, Int. J. Model. Simul. Sci. Comput. 4(2013), 1250030.

[13] Jha BK, Adlakha N, Mehta MN, Two-dimensional finite element model to study calcium distribution in astrocytes in presence of excess buffer, Int. J. Biomath. 7(2014), 1450031.

[14] Manhas N, Pardasani KR, Mathematical model to study IP3 dynamics dependent calcium oscillations in pancreatic acinar cells, J. Med. Imaging Health Inf. 4(2014), 874-880.

[15] Manhas N, Pardasani KR, Modelling mechanism of calcium oscillations in pancreatic acinar cells, J. Bioenerg. Biomembranes, 46(2014), 403-420.

[16] Manhas N, Sneyd J, Pardasani KR, Modelling the transition from simple to complex Ca2+ oscillations in pancreatic acinar cells, J. Biosci. 39(2014), 463-484.

[17] Naik PA, Pardasani KR, One Dimensional Finite Element Model to Study Calcium Distribution in Oocytes in Presence of VGCC, RyR and Buffers, J. Med. Imaging Health Inf. 5(2015), 471-476.

[18] Naik PA, Pardasani KR, One dimensional finite element method approach to study effect of ryanodine receptor and serca pump on calcium distribution in oocytes, J. Multiscale Model. 5(2013), 1350007.

[19] Panday S, Pardasani KR, Finite element model to study the mechanics of calcium regulation in oocyte, J. Mech. Med. Biol. 14(2014), Article ID 1450022.

[20] Pathak K, Adlakha N, Finite Element Model to Study Calcium Signaling in Cardiac Myocytes Involving Pump, Leak and Excess Buffer, J. Med. Imaging Health Inf. 5(2015), 1-6.

[21] Pathak K, Adlakha N, Finite element model to study two dimensional unsteady state calcium distribution in cardiac myocytes, Alexandria J. Med. 52(2016), 261-268.

[22] De Y, Gary W, Keizer J, A single-pool inositol 1, 4, 5-trisphosphate-receptor-based model for agonist-stimulated oscillations in Ca2+ concentration, Proc. Natl. Acad. Sci. 89(1992), 9895-9899.

[23] Versteeg HK, Malalasekera W, An introduction to computational fluid dynamics: the finite volume method, Pearson Education, (2007).